# Robust recovery of low-rank matrices and low-tubal-rank tensors from noisy sketches\*

Anna Ma<sup>†</sup> Dominik Stöger<sup>‡</sup> Yizhe Zhu<sup>§</sup>

June 6, 2022

#### Abstract

A common approach for compressing large-scale data is through matrix sketching. In this work, we consider the problem of recovering low-rank matrices from two noisy sketches using the double sketching algorithm discussed in Fazel et al. (2008). Using tools from non-asymptotic random matrix theory, we provide the first theoretical guarantees characterizing the error between the output of the double sketch algorithm and the ground truth low-rank matrix. We apply our result to the problems of low-rank matrix approximation and low-tubal-rank tensor recovery.

## 1 Introduction

The prevalence of large-scale data in data science applications has created immense demand for methods that can aid in reducing the computational cost of processing and storing said data. Oftentimes, data such as images, videos, and text documents, can be represented as a matrix, and thus, the ability to efficiently store matrices becomes an important task. One way to efficiently store a large-scale matrix  $X \in \mathbb{R}^{m \times n}$  is to store a *sketch* of the matrix, i.e., another matrix  $Y \in \mathbb{R}^{m_1 \times n_1}$  such that two goals are accomplished. Firstly, the sketch of X must be cheaper to store than X itself, i.e., we want  $m_1 n_1 \ll mn$ . Second, the matrix X must be recoverable from its sketch.

A variety of works have been produced for the setting in which X is a low-rank matrix, and one wishes to recover X using its sketch [13, 26]. However, in certain settings, one may only have access to noisy sketches. For example, suppose a sketch Y is stored on a hard disk drive. Over time, the hard drive experiences data degradation due to bits losing their magnetic orientation or extreme fluctuations in temperature affecting the physical hard drive itself [12]. As another example, the matrix being sketched can be a noisy version of the data one is trying to preserve [4]. One can even consider the low-rank approximation problem as one such instance.

In this work, we analyze the noisy double-sketch algorithm originally proposed but not theoretically studied in [13]. We show that when the sketching matrices are i.i.d. complex Gaussian random matrices, one can recover the original low-rank matrix X with high probability where the error on the approximation depends on the noise level for both sketches. Here, we do not assume that one has access to the exact rank of X but instead an approximate rank  $r > r_0$ . We also remark on the utility of our theoretical guarantees

<sup>\*</sup>A.M. was supported by U.S. Air Force Grant FA9550-18-1-0031, NSF Grant DMS 2027299, and the NSF+Simons Research Collaborations on the Mathematical and Scientific Foundations of Deep Learning. Y.Z. was partially supported by NSF-Simons Research Collaborations on the Mathematical and Scientific Foundations of Deep Learning. Y.Z. also acknowledges support from NSF DMS-1928930 during his participation in the program "Universality and Integrability in Random Matrix Theory and Interacting Particle Systems" hosted by the Mathematical Sciences Research Institute in Berkeley, California, during the Fall semester of 2021.

<sup>&</sup>lt;sup>†</sup>Department of Mathematics, University of California Irvine (anna.ma@uci.edu).

<sup>&</sup>lt;sup>‡</sup>Department of Mathematics and Mathematical Institute for Machine Learning and Data Science (MIDS), KU Eichstätt-Ingolstadt (dominik.stoeger@ku.de).

<sup>§</sup>Department of Mathematics, University of California Irvine (yizhe.zhu@uci.edu).

for when the double sketch algorithm is used not for low-rank matrix recovery but instead for low-rank approximation with noise. Lastly, we present results for the application of this work to a more extreme large-scale data setting in which one wants to recover a low-tubal-rank tensor.

A key step in our robust recovery analysis is to control the perturbation error of a low-rank matrix under noise. A standard way is to apply Wedin's theorem, or Davis-Kahan theorem [34, 8, 7, 22] which results in a bound that depends on the condition number of the low-rank matrix. However, our proof is based on an exact formula to calculate the difference between output and the ground truth matrix and a detailed analysis of the random matrices (extreme singular value bounds of Gaussian matrices [32, 25, 28] and the least singular value of truncated Haar unitary matrices [3, 9]) involved in the double sketch algorithm. This novel approach yields a bound independent of the condition number of the low-rank matrix (Theorem 2). Due to the Gaussian structure of our sensing matrices, our results are non-asymptotic, and all the constants involved in the probabilistic error bounds are explicit.

## 1.1 Low-rank matrix recovery

A double sketching algorithm was proposed in [13] to recover low-rank matrices. This approach was also called bilateral random projection and analyzed in [40] to obtain a low-rank approximation of matrix X using two sketched matrices from X in the noiseless situation. A similar approach was analyzed in [29]. The so-called problem of compressive PCA was studied in [26] and [1]. It can be interpreted as a variant of sketching where only the columns of a matrix are sketched. However, this problem is not directly comparable to the setting in the paper at hand, as in compressive PCA, a different sketching matrix is used for each column.

#### 1.2 Low-tubal-rank tensor recovery

The notion of a low-tubal-rank tensor stems from the t-product, originally introduced by [18]. We state the relevant definitions for order-3 tensors, and more general definitions for tensors of higher orders can be found in [17, 19].

**Definition 1** (Operations on tensors). Let  $A \in \mathbb{C}^{n_1 \times n_2 \times n_3}$ . The unfold of a tensor is defined to be the frontal slice stacking of that tensor. In other words,

$$unfold(\mathcal{A}) = \begin{pmatrix} A_1 \\ A_2 \\ \vdots \\ A_{n_3} \end{pmatrix} \in \mathbb{C}^{n_1 n_3 \times n_2},$$

where  $A_i = \mathcal{A}_{:,:,i}$  denotes the  $i^{th}$  frontal slice of  $\mathcal{A}$ . We define the inverse of the unfold(·) as fold(·) so that  $fold(unfold(\mathcal{A})) = \mathcal{A}$ . The block circulant matrix of  $\mathcal{A}$  is:

$$bcirc(\mathcal{A}) = \begin{pmatrix} A_1 & A_{n_3} & A_{n_3-1} & \dots & A_2 \\ A_2 & A_1 & A_{n_3} & \dots & A_3 \\ \vdots & \vdots & \vdots & \ddots & \vdots \\ A_{n_3} & A_{n_3-1} & A_{n_3-2} & \dots & A_1 \end{pmatrix} \in \mathbb{C}^{n_1 n_3 \times n_2 n_3}.$$

The conjugate transpose of a tensor  $A \in \mathbb{C}^{n_1 \times n_2 \times n_3}$  is the tensor  $A^* \in \mathbb{C}^{n_2 \times n_1 \times n_3}$  obtained by conjugate transposing each of the frontal slice and then reversing the order of transposed frontal slices 2 through  $n_3$ .

**Definition 2** (Tensor t-product). Let  $A \in \mathbb{C}^{n_1 \times \ell \times n_3}$  and  $B \in \mathbb{C}^{\ell \times n_2 \times n_3}$  then the t-product between A and B, denoted A \* B, is a tensor of size  $n_1 \times n_2 \times n_3$  as is computed as:

$$A * B = fold(bcirc(A)unfold(B)). \tag{1}$$

**Definition 3** (Mode-3 fast Fourier transformation (FFT)). The mode-3 FFT of a tensor  $\mathcal{A}$ , denoted  $\widehat{\mathcal{A}}$ , is obtained by applying the discrete Fourier Transform matrix,  $F \in \mathbb{C}^{n_3 \times n_3}$ , to each  $\mathcal{A}_{i,j,:}$  of  $\mathcal{A}$ :

$$\widehat{\mathcal{A}}_{i,j,:} = F \mathcal{A}_{i,j,:}. \tag{2}$$

Here, F is a unitary matrix,  $A_{i,j,:}$  is an  $n_3$ -dimensional vector, and the product is the usual matrix-vector product.

**Definition 4** (t-SVD). The Tensor Singular Value Decomposition (t-SVD) of a tensor  $\mathcal{M} \in \mathbb{C}^{n_1 \times n_2 \times n_3}$  is given by

$$\mathcal{M} = \mathcal{U} * \mathcal{S} * \mathcal{V}^*, \tag{3}$$

where  $\mathcal{U} \in \mathbb{C}^{n_1 \times n_1 \times n_3}$  and  $\mathcal{V} \in \mathbb{C}^{n_2 \times n_2 \times n_3}$  are unitary tensors and  $\mathcal{S} \in \mathbb{R}^{n_1 \times n_2 \times n_3}$  is a tubal tensor (a tensor in which each frontal slice is diagonal), and \* denotes the t-product.

**Definition 5** (Tubal rank). The tubal rank of a tensor  $\mathcal{M} = \mathcal{U} * \mathcal{S} * \mathcal{V}^*$  is the number of non-zero singular tubes of  $\mathcal{S}$ .

**Definition 6** (CP rank). The CP rank of an order three tensor  $\mathcal{M}$  is the smallest integer r such that  $\mathcal{M}$  is a sum of rank-1 tensor:

$$\mathcal{M} = \sum_{i=1}^{r} u_i \otimes v_i \otimes w_i,$$

where  $u_i \in \mathbb{C}^{n_1}, v_i \in \mathbb{C}^{n_2}, w_i \in \mathbb{C}^{n_3}, 1 \leq i \leq r$ .

**Remark 1.** If a tensor  $\mathcal{M}$  has CP rank r then its tubal rank is at most r, see [39, Remark 2.3].

**Definition 7** (Tensor Frobenius norm). Let  $\mathcal{M} \in \mathbb{C}^{n_1 \times n_2 \times n_3}$ . The Frobenius norm of  $\mathcal{M}$  is given by

$$\|\mathcal{M}\|_F = \left(\sum_{i_1, i_2, i_3} |\mathcal{M}_{i_1, i_2, i_3}|^2\right)^{1/2}.$$

Other low-rank tensor sketching approaches have been proposed for low-CP-rank tensors [16] and low-Tucker-rank tensors [27]. In the following, we focus on low-tubal-rank tensors since this is the topic of this paper.

In the related line of work [20, 38, 37], the authors consider recovering low-tubal-rank tensors through general linear Gaussian measurements of the form y = A vec(X). This can be seen as a generalization of the low-rank matrix recovery problem [24] to low-tubal-rank tensors. The proof of tensor recovery under Gaussian measurements in [20, 38, 37] relies crucially on the assumption that the entries of the measurement matrix A are i.i.d. Gaussian. In this setting, it was shown that the tensor nuclear norm is an atomic norm, and a general theorem from [6, Corollary 12] for i.i.d. measurements for atomic norms was used to establish recovery guarantees. In [33] a non-convex surrogate for the tensor nuclear norm was proposed and studied.

An extension of the matrix sketching algorithm in [30] to a low-tubal-rank approximation of tensors was considered in [23]. However, their setting does not cover noisy sketching, which is the topic of this paper. Streaming low-tubal-rank tensor approximation was considered in [36].

Notations We define a standard complex Gaussian random variable **Z** as  $\mathbf{Z} = \mathbf{X} + i\mathbf{Y}$ , where  $\mathbf{X} \sim N(0, 1/2)$ ,  $\mathbf{Y} \sim N(0, 1/2)$  and  $\mathbf{X}$ ,  $\mathbf{Y}$  are independent. By  $\sigma_i(A)$  we define the *i*-th largest singular value of a matrix A. By  $\sigma_{\min}(A)$  we denote the smallest non-zero singular value of a matrix A.  $||A||_{2\to 2}$  is the spectral norm of a matrix A, and ||A|| is a general norm of A.  $A^*$  is the complex conjugate, and  $A^{\dagger}$  is the pseudo-inverse of A. Let A0 be a matrix with orthonormal columns. A1 is the orthogonal complement of A2, which means the column vectors of A3 and the column vectors of A4 form a complete orthonormal basis.

**Organization of the paper** The rest of the paper is organized as follows. We state our main results and corollaries of robust recovery of low-rank matrix and low-tubal-rank tensors in Section 2. The proof of all theorems and corollaries are given in Section 3, and auxiliary lemmas are provided in Appendix.

## 2 Main Results

## 2.1 Low-rank matrix recovery

Let  $X_0 \in \mathbb{C}^{n_1 \times n_2}$  be a matrix of rank  $r_0$ .  $S \in \mathbb{C}^{r \times n_1}$ ,  $\tilde{S} \in \mathbb{C}^{r \times n_2}$  be two independent complex Gaussian random matrices with  $r \geq r_0$ . Define

$$Y = SX_0 + Z, \quad \tilde{Y} = \tilde{S}X_0^* + \tilde{Z}, \tag{4}$$

where  $Z \in \mathbb{C}^{r \times n_2}$ ,  $\tilde{Z} \in \mathbb{C}^{r \times n_1}$  are of full rank, and  $\tilde{Z}$  is independent of S. The double sketch algorithm outputs

$$X = \tilde{Y}^* (S\tilde{Y}^*)^{\dagger} Y. \tag{5}$$

When  $Z, \tilde{Z} = 0$ , we denote the output of (5) as  $\overline{X}$ . In this case, the output will be

$$\overline{X} = X_0 \tilde{S}^* (SX_0 \tilde{S}^*)^{\dagger} SX_0. \tag{6}$$

We first show that without noise, the algorithm exactly recovers  $X_0$ , i.e.,  $\overline{X} = X_0$  with probability 1.

**Theorem 1** (Exact recovery). Let  $S \in \mathbb{C}^{r \times n_1}$ ,  $\tilde{S} \in \mathbb{C}^{r \times n_2}$  be two independent complex standard Gaussian random matrices. Furthermore, let  $X_0 \in \mathbb{C}^{n_1 \times n_2}$  be a matrix with rank  $r_0$ . If  $r \geq r_0$  and  $Z, \tilde{Z} = 0$  then with probability one  $\overline{X} = X_0$ , where  $\overline{X}$  is as defined in (6).

Our Theorem 1 generalized the exact recovery result [13, Lemma 6], where r is assumed to be exactly  $r_0$ . Our Theorem 1 implies the exact value of  $r_0$  is not needed for the double sketch algorithm, and one can always use the parameter  $r \geq r_0$ . In fact, our robust recovery result (Theorem 2) suggest choosing a larger r makes the output of the double sketch algorithm more robust to noise.

When  $Z, \tilde{Z}$  are not all zero, the robust recovery guarantee is given as follows.

**Theorem 2** (Robust recovery). Assume  $r_0 < r < n_1$ ,  $\tilde{Y}$  is of rank r and  $\tilde{Z}$  is independent of S. For any  $\delta_1, \delta_2, \varepsilon > 0$ , with probability at least  $1 - \delta_1 - \delta_2 - \varepsilon$ , the output X from the double sketch algorithm given in (5) satisfies

$$|||X - X_0||| \le \frac{\sqrt{r(n_1 - r)} |||\tilde{Z}|||}{\sqrt{\delta_1}(\sqrt{r} - \sqrt{r_0} - \sqrt{\log(1/\delta_2)})} + \frac{\sqrt{r}|||Z|||}{\sqrt{\log(1/(1 - \varepsilon))}},$$

where  $\|\cdot\|$  is any matrix norm that satisfies for any two matrices A and B,  $\|AB\| \le \|A\|_{2\to 2} \|B\|$ , and  $\|A\| = \|A^*\|$ . In particular, it holds for  $\|\cdot\|_{2\to 2}$  and  $\|\cdot\|_F$ .

**Remark 2.** The condition that  $\tilde{Y}$  is of rank r can be easily verified in different settings. For example, it holds when  $\tilde{Z}$  is independent of  $\tilde{S}$ , or  $\tilde{Y} = \tilde{S}(X_0^* + \hat{Z})$ , where  $X_0^* + \hat{Z}$  is of full rank. In the second case, when  $\hat{Z}$  is a matrix with independent entries generated from a continuous distribution, we cover "low-rank plus noise" sketching.

**Remark 3.** Our proof of Theorem 2 works for  $r = r_0$  or  $r = n_1$ , but the error bounds are slightly different.

• When  $r = r_0 < n_1$ , (14) is replaced by the estimate that  $\sigma_{\min}(\tilde{S}V_0) \ge \sqrt{\log(1/(1-\delta_2))}r^{-1/2}$  with probability  $1 - \delta_2$ . This implies with probability at least  $1 - \delta_1 - \delta_2 - \varepsilon$ ,

$$|||X - X_0||| \le \frac{r\sqrt{n_1 - r}||\tilde{Z}||}{\sqrt{\delta_1}(\log(1/(1 - \delta_2))} + \frac{\sqrt{r}||Z||}{\sqrt{\log(1/(1 - \varepsilon))}}.$$

• When  $r = n_1$ ,  $U_A$  defined in (8) is a unitary matrix and S is invertible. We find  $\tilde{X} = X_0$  in (11) and following the rest of the proof we obtain with probability at least  $1 - \varepsilon$ ,

$$|||X - X_0||| \le \frac{\sqrt{n_1} |||Z|||}{\sqrt{\log(1/(1-\varepsilon))}}.$$

## 2.2 Low-rank matrix approximation

When  $X_0$  is not low-rank, we can write  $X_0 = X_1 + E$ , where  $X_1$  is the best rank- $r_1$  approximation of  $X_0$ . Letting  $r_0 > r > r_1$ , we can use the noisy double sketch model in (4) to consider the sketches

$$Y = SX_0 + Z = SX_1 + (SE + Z),$$
  
 $\tilde{Y} = \tilde{S}X_0^* + \tilde{Z} = \tilde{S}X_1^* + (\tilde{S}E + \tilde{Z}).$ 

When  $Z = \tilde{Z} = 0$ , such a problem was considered in [13, 35] using the double sketch algorithm and an extra step of truncated r-term SVD of Y and  $\tilde{Y}$ . See [13] for more details. The noiseless version of the algorithm was also analyzed in [29] and a power scheme modification of the algorithm was analyzed in [40]. In the noiseless setting, a direct application of the double sketch algorithm without the truncation steps yields a weaker error bound from Corollary 1 when compared to [29]. We can handle noise in the double sketch, while the proofs from [29, 40] are not applicable. The proofs in [29, 40] heavily rely on the assumption  $Z = \tilde{Z} = 0$  to use properties of orthogonal projections, which only hold in this noiseless scenario. See for example [29, Fact A.2]. The proof of Corollary 1 is given in Section 3.3.

Corollary 1 (Low-rank approximation with noisy sketch). Let  $X_0 \in \mathbb{C}^{n_1 \times n_2}$ . Let  $r_1$  be an integer such that  $r_1 < r < n_1$ . Consider the algorithm

$$Y = SX_0 + Z, \quad \tilde{Y} = \tilde{S}X_0^* + \tilde{Z}, \quad X = \tilde{Y}^*(S\tilde{Y}^*)^{\dagger}Y.$$

Suppose  $\tilde{Y}$  is of rank r. For any  $\delta_1, \varepsilon > 0$  and  $\delta_2 > \exp(-(\sqrt{r} - \sqrt{r_1})^2)$ , with probability at least  $1 - \delta_1 - 3\delta_2 - \varepsilon$ , the output X satisfies

$$\|X - X_0\|_{2\to 2} \le \sigma_{r_1+1}.$$

$$\left( \frac{\sqrt{r(n_1 - r)}(\sqrt{r} + \sqrt{n_2} + \sqrt{\log(1/\delta_2)})}{\sqrt{\delta_1}(\sqrt{r} - \sqrt{r_1} - \sqrt{\log(1/\delta_2)})} + \frac{\sqrt{r}\left(\sqrt{r} + \sqrt{n_1} + \sqrt{\log(1/\delta_2)}\right)}{\sqrt{\log(1/(1 - \varepsilon))}} + 1 \right)$$

$$+ \frac{\sqrt{r(n_1 - r)} \|\tilde{Z}\|_{2\to 2}}{\sqrt{\delta_1}(\sqrt{r} - \sqrt{r_1} - \sqrt{\log(1/\delta_2)})} + \frac{\sqrt{r}\|Z\|_{2\to 2}}{\sqrt{\log(1/(1 - \varepsilon))}}.$$

**Remark 4.** Although our error bound depends on  $\sigma_{r_1+1}$ , the output X is a rank-r approximation of the ground truth matrix  $X_0$ . This bound is true for any  $r_1 < r$ . Therefore one can optimize  $r_1$  to find the best bound in terms of the failure probability and the approximation error.

## 2.3 Application to sketching low-tubal-rank tensors

The approach set forth in (5) can be used to sketch and recover low-tubal-rank tensors. For such an application, one considers the low-tubal-rank tensor  $\mathcal{X} \in \mathbb{R}^{n_1 \times n_2 \times n_3}$  with tubal rank r. Taking the mode-3 FFT of  $\mathcal{X}$ , one obtains  $\hat{\mathcal{X}}$  which is composed of a collection of  $n_3$  matrices (frontal slices) of dimension  $n_1 \times n_2$  with rank at most r. As such, (5) can be used to sketch each of the  $n_3$  frontal slices of  $\mathcal{X}$ . Corollary 2 captures the approximation error for such an approach, and its proof is given in Section 3.3.

Corollary 2 (Recovering low tubal-rank tensors). Let  $\mathcal{X}_0 \in \mathbb{C}^{n_1 \times n_2 \times n_3}$  be a low-tubal-rank tensor with rank  $r_0$ . Furthermore, let  $r_0 < r < n_1$ ,  $S \in \mathbb{C}^{r \times n_1}$ ,  $\tilde{S} \in \mathbb{C}^{r \times n_2}$  be two independent complex standard Gaussian random matrices. Consider the measurements

$$\mathcal{Y} = \mathcal{S} * \mathcal{X}_0 + \mathcal{Z}, \ \tilde{\mathcal{Y}} = \tilde{\mathcal{S}} * \mathcal{X}_0^* + \tilde{\mathcal{Z}},$$
 (7)

where  $S_1 = S$ ,  $\tilde{S}_1 = \tilde{S}$  and  $S_k = \tilde{S}_k = 0$  for all  $k \in \{2, ..., n_3\}$ .

- 1. (Exact Recovery) If  $\mathcal{Z} = \mathbf{0}$  and  $\tilde{\mathcal{Z}} = \mathbf{0}$  then with probability 1,  $\mathcal{X} = \mathcal{X}_0$ .
- 2. (Robust Recovery) If for all  $k \in [n_3]$ ,  $\mathcal{Y}_k = S\hat{\mathcal{X}}_{0k} + \mathcal{Z}_k$  is of rank r, then for any  $\delta_1, \varepsilon > 0$ , and  $\delta_2 > \exp(-(\sqrt{r} \sqrt{r_1})^2)$ , with probability at least  $1 (\delta_1 + \delta_2 + \varepsilon)n_3$ ,

$$\|\mathcal{X} - \mathcal{X}_0\|_F^2 \le \frac{2r(n_1 - r)\|\tilde{\mathcal{Z}}\|_F^2}{\delta_1(\sqrt{r_1} - \sqrt{r} - \sqrt{\log(1/\delta_2)})^2} + \frac{2r\|\mathcal{Z}\|_F^2}{\log(1/(1 - \varepsilon))}.$$

**Remark 5.** In the closely related work [23], the authors considered low-tubal-rank tensor approximation from noiseless sketches, extending the results from [29], while our setting here is to recover low-tubal-rank tensors from noisy sketches. In addition, [23] requires two sketching tensors  $S, \tilde{S}$  with i.i.d. Gaussian entries in the sketching procedure, whereas here we only require two sensing matrices S and  $\tilde{S}$  with independent Gaussian entries to sketch the low-tubal-rank tensors.

## 3 Proof of main results

Our proof for robust matrix recovery, presented in Theorem 2, derives an upper bound for the difference between the output X and the ground truth matrix  $X_0$ . To accomplish this, the approximation error,  $X - \tilde{X}_0$ , is decomposed into two components. The first part depends on  $\tilde{Z}$  and can be written as  $PX_0$  for a projection matrix P, and we used the oblique projection matrix expression in Lemma 3 to simplify the expression. We then control the error by relating it to the smallest singular value of a truncated Haar unitary matrix. Here we use the crucial fact that when  $\tilde{Y}$  is full-rank,  $\text{Im}(P) = \ker S$  is uniformly distributed on the Grassmannian of all (n-r)-dimensional subspaces in  $\mathbb{C}^n$ . When  $\tilde{Y}$  is not full rank, Im(P) does not have such nice property, and our proof technique cannot be directly applied. This part of the proof is summarized in Lemma 1.

The second part of the component in the decomposition of the error depends on Z is simpler to handle. For this part, a lower bound on the smallest singular value of Gaussian random matrices is utilized.

**Remark 6.** The distribution of the smallest singular value of truncated Haar unitary matrices was explicitly calculated in [9, 3]. For a more general class of random matrices (including Haar orthogonal matrices), such a distribution was derived in [9, 11, 2] in terms of generalized hypergeometric functions. By using the corresponding tail probability bound [2, Corollary 3.4] for truncated Haar orthogonal matrices, our analysis can be extended to real Gaussian sketching matrices S and  $\tilde{S}$ .

#### 3.1 Proof of Theorem 1

*Proof.* Let  $X_0 = U_0 \Sigma_0 V_0^*$  be the SVD of  $X_0$  where  $U_0$  is  $n_1 \times r_0$ ,  $V_0$  is  $n_2 \times r_0$  and  $\Sigma_0$  is an invertible, diagonal  $r_0 \times r_0$  matrix. Now we can write  $\overline{X}$  as

$$\overline{X} = U_0 \Sigma_0 V_0^* \tilde{S}^* (SU_0 \Sigma_0 V_0^* \tilde{S}^*)^{\dagger} SU_0 \Sigma_0 V_0^*.$$

Note that since  $S, \tilde{S}$  are Gaussian matrices and since  $U_0$  and  $V_0$  are orthonormal,  $SU_0 \in \mathbb{C}^{r \times r_0}$  and  $\tilde{S}V_0 \in \mathbb{C}^{r \times r_0}$  have linearly independent columns with probability 1 and by Lemma 2,

$$(SU_0)^{\dagger}SU_0 = I, \quad V_0^* \tilde{S}^* (V_0^* \tilde{S}^*)^{\dagger} = I.$$

So with probability 1,

$$\overline{X} = U_0 \Sigma_0 V_0^* \tilde{S}^* (V_0^* \tilde{S}^*)^{\dagger} \Sigma_0^{-1} (SU_0)^{\dagger} (SU_0) \Sigma_0 V_0^* = U_0 \Sigma V_0^* = X_0.$$

## 3.2 Proof of Theorem 2

The double sketch algorithm outputs

$$X = \tilde{Y}^* (S\tilde{Y}^*)^{-1} (SX_0 + Z) = \tilde{X} + \tilde{Y}^* (S\tilde{Y}^*)^{-1} Z$$

where  $\tilde{X} := \tilde{Y}^* (S\tilde{Y}^*)^{-1} SX_0$ .

Let A be such that

$$A := \tilde{Z}^* + X_0 \tilde{S}^* \in \mathbb{C}^{n_1 \times r}.$$

Since  $A = \tilde{Y}^*$  is of rank r from the assumption in Theorem 2, we denote the SVD of A as

$$A = U_A \Sigma_A V_A^*,$$

$$U_A \in \mathbb{C}^{n_1 \times r}, \Sigma_A \in \mathbb{C}^{r \times r}, V_A \in \mathbb{C}^{r \times r}.$$
(8)

Furthermore, since S and  $\tilde{Z}$  are independent,  $SU_A$  is invertible with probability 1. Therefore,

$$\tilde{Y}^*(S\tilde{Y}^*)^{\dagger} = A(SA)^{\dagger}$$

$$= (U_A \Sigma_A V_A^*) (SU_A \Sigma_A V_A^*)^{\dagger}$$

$$= U_A \Sigma_A V_A^* V_A \Sigma_A^{-1} (SU_A)^{-1}$$

$$= U_A (SU_A)^{-1}.$$
(9)

Using this notation, the output of (5) simplifies to

$$X = \tilde{X} + \tilde{Y}^* (S\tilde{Y}^*)^{-1} Z = \tilde{X} + U_A (SU_A)^{-1} Z.$$

Then

$$X - X_0 = \tilde{X} - X_0 + \tilde{Y}^* (S\tilde{Y}^*)^{-1} Z = (\tilde{X} - X_0) + U_A (SU_A)^{-1} Z,$$

and since our goal is to bound the approximation error, we consider

$$|||X - X_0||| \le |||\tilde{X} - X_0||| + |||U_A(SU_A)^{-1}Z|||.$$

Lemma 1 allows us to bound the first term in this inequality.

**Lemma 1.** If Z = 0, then with probability at least  $1 - \delta_1 - \delta_2$  with  $\delta_1 > 0, \delta_2 > \exp(-(\sqrt{r} - \sqrt{r_1})^2)$ , the output  $\tilde{X}$  of the algorithm in (5) satisfies

$$\|\tilde{X} - X_0\| \le \frac{\sqrt{r(n_1 - r)} \|\tilde{Z}\|}{\sqrt{\delta_1}(\sqrt{r} - \sqrt{r_0} - \sqrt{\log(1/\delta_2)})}.$$
(10)

*Proof.* From (9) and Theorem 1,

$$\tilde{X} - X_0 = \tilde{Y}^* (S\tilde{Y}^*)^{\dagger} S X_0 - X_0 
= U_A (SU_A)^{-1} S X_0 - X_0 
= -(I - U_A (SU_A)^{-1} S) X_0 
= -P X_0.$$
(11)

where we have set  $P := I - U_A(SU_A)^{-1}S$ . We observe that P is a projection, i.e.  $P^2 = P$  which satisfies

$$\ker P = U_A,$$

Im 
$$P = \ker S =: \tilde{V} \in \mathbb{C}^{n_1 \times (n_1 - r)}$$
.

Recall that  $X_0 = U_0 \Sigma_0 V_0^*$  is the SVD of  $X_0$ . From Lemma 3,

$$PX_0 = \tilde{V}(U_{A,\perp}^* \tilde{V})^{-1} U_{A,\perp}^* X_0$$
  
=  $\tilde{V}(U_{A,\perp}^* \tilde{V})^{-1} U_{A,\perp}^* U_0 \Sigma_0 V_0^*$ .

Then we can bound

$$\|\tilde{X} - \overline{X}\| = \|\tilde{V}(U_{A,\perp}^* \tilde{V})^{-1} U_{A,\perp}^* U_0 \Sigma_0 V_0^* \|$$

$$\leq \|(U_{A,\perp}^* \tilde{V})^{-1}\|_{2 \to 2} \|U_{A,\perp}^* U_0 \Sigma_0 V_0^* \|. \tag{12}$$

We focus our efforts on simplifying the second term of (12). Writing A in terms of the SVD of  $X_0$ , one obtains

$$A = \tilde{Z}^* + X_0 \tilde{S}^* = U_A \Sigma_A V_A^* = \tilde{Z} + U_0 \Sigma_0 V_0^* \tilde{S}^*.$$

Rearranging terms yields

$$U_0 \Sigma_0 V_0^* \tilde{S}^* = A - \tilde{Z}^*.$$

Since  $\tilde{S}V_0$  is of size  $r \times r_0$ ,  $\tilde{S}$  is complex Gaussian and  $V_0$  has orthonormal columns, then from Lemma 2, with probability 1,  $\tilde{S}V_0$  has linearly independent columns. Thus  $V_0^*\tilde{S}^*$  has linearly independent rows and

$$(V_0^* \tilde{S}^*)(V_0^* \tilde{S}^*)^{\dagger} = I.$$

This implies that

$$U_0 \Sigma_0 = \left( A - \tilde{Z}^* \right) \left( V_0^* \tilde{S}^* \right)^{\dagger}.$$

We note that

$$\begin{split} \| U_{A,\perp}^* U_0 \Sigma_0 V_0^* \| &= \| U_{A,\perp}^* U_0 \Sigma_0 \| \\ &= \| U_{A,\perp}^* \left( A - \tilde{Z}^* \right) \left( V_0^* \tilde{S}^* \right)^\dagger \| \\ &= \| U_{A,\perp}^* \tilde{Z}^* \left( V_0^* \tilde{S}^* \right)^\dagger \| \\ &\leq \| U_{A,\perp}^* \tilde{Z}^* \| \| \left( V_0^* \tilde{S}^* \right)^\dagger \|_{2 \to 2} \\ &= \frac{\| U_{A,\perp}^* \tilde{Z}^* \|}{\sigma_{\min} \left( V_0^* \tilde{S}^* \right)} \leq \frac{\| \tilde{Z} \|}{\sigma_{\min} \left( V_0^* \tilde{S}^* \right)}. \end{split}$$

Using the fact that  $\|(U_{A,\perp}^*\tilde{V})^{-1}\| = 1/\sigma_{\min}(U_{A,\perp}^*\tilde{V})$  for the first term of (12), we then obtain the following bound:

$$\|\tilde{X} - \overline{X}\| \le \frac{\|\tilde{Z}\|}{\sigma_{\min}(U_{A,\perp}^* \tilde{V}) \sigma_{\min}\left(\tilde{S}V_0\right)},\tag{13}$$

which holds with probability 1.

We now derive a probabilistic bound from (13) using concentration inequalities from random matrix theory. Since  $\tilde{V}$  can be seen as the  $n_1 \times (n_1 - r)$  submatrix of a Haar unitary matrix  $(\tilde{V}, \tilde{V}_{\perp})$ . By unitary invariance property,

$$M := \begin{bmatrix} U_{A,\perp}^* \\ U_A^* \end{bmatrix} (\tilde{V}, \tilde{V}_\perp)$$

is also a Haar unitary matrix, and  $U_{A,\perp}^* \tilde{V}$  is exactly the upper left  $(n_1 - r) \times (n_1 - r)$  corner of M. We can apply Lemma 4 to get

$$\mathbb{P}\left(\|(U_{A,\perp}^*\tilde{V})^{-1}\| \le \frac{\sqrt{r(n_1-r)}}{\sqrt{\delta_1}}\right) \ge 1 - \delta_1$$

for any  $\delta_1 > 0$ . Since  $\tilde{S}V_0$  is distributed as a  $r \times r_0$  complex Gaussian random matrix, if  $r > r_0$ , by Lemma 5, for any  $\delta_2 > 0$ , with probability at least  $1 - \delta_2$ ,

$$\sigma_{\min}(\tilde{S}V_0) \ge \sqrt{r} - \sqrt{r_0} - \sqrt{\log(1/\delta_2)}. \tag{14}$$

Combining the two probability estimates, with probability at least  $1 - \delta_1 - \delta_2$ ,

$$\|\tilde{X} - \overline{X}\| \le \frac{\sqrt{r(n_1 - r)} \|\tilde{Z}\|}{\sqrt{\delta_1}(\sqrt{r} - \sqrt{r_0} - \sqrt{\log(1/\delta_2)})}.$$

For the second term, by the independence between S and  $\tilde{Z}$ ,  $SU_A$  is distributed as an  $r \times r$  standard complex Gaussian matrix it follows from Lemma 6 that with probability at least  $1 - \varepsilon$ ,

$$\sigma_{\min}(SU_A) \ge \sqrt{\log(1/(1-\varepsilon))}r^{-1/2}$$
.

Thus, with probability at least  $1 - \varepsilon$ .

$$|||U_{A}(SU_{A})^{-1}Z||| \leq ||U_{A}||_{2\to 2}||(SU_{A})^{-1}||_{2\to 2}||Z||$$

$$= \frac{1}{\sigma_{\min}(SU_{A})}||Z||$$

$$\leq \frac{\sqrt{r}}{\sqrt{\log(1/(1-\varepsilon))}}|||Z|||.$$
(15)

Combining (10) and (15) yields the desired result.

## 3.3 Proof of Corollaries

Proof of Corollary 1. Write  $X_0 = X_1 + E$ , where  $X_1$  is the best rank- $r_1$  approximation to  $X_0$ . We obtain

$$Y = SX_0 + Z = SX_1 + (SE + Z),$$
  
 $\tilde{Y} = \tilde{S}X_0^* + \tilde{Z} = \tilde{S}X_1^* + (\tilde{S}E + \tilde{Z}).$ 

Applying Theorem 2 to  $X_1$  and two error terms (SE+Z) and  $\tilde{S}E+\tilde{Z}$ , the following error bound holds with probability at least  $1-\delta_1-\delta_2-\varepsilon$ ,

$$\begin{split} &\|X - X_0\|_{2 \to 2} \le \|X - X_1\|_{2 \to 2} + \|E\|_{2 \to 2} \\ &\le \frac{\sqrt{r(n_1 - r)} \|\tilde{S}E + \tilde{Z}\|_{2 \to 2}}{\sqrt{\delta_1}(\sqrt{r} - \sqrt{r_1} - \sqrt{\log(1/\delta_2)})} + \frac{\sqrt{r} \|SE + Z\|_{2 \to 2}}{\sqrt{\log(1/(1 - \varepsilon))}} + \|E\|_{2 \to 2} \\ &\le \left(\frac{\sqrt{r(n_1 - r)} \|\tilde{S}\|_{2 \to 2}}{\sqrt{\delta_1}(\sqrt{r} - \sqrt{r_1} - \sqrt{\log(1/\delta_2)})} + \frac{\sqrt{r} \|S\|_{2 \to 2}}{\sqrt{\log(1/(1 - \varepsilon))}} + 1\right) \|E\|_{2 \to 2} \\ &+ \frac{\sqrt{r(n_1 - r)} \|\tilde{Z}\|_{2 \to 2}}{\sqrt{\delta_1}(\sqrt{r} - \sqrt{r_1} - \sqrt{\log(1/\delta_2)})} + \frac{\sqrt{r} \|Z\|_{2 \to 2}}{\sqrt{\log(1/(1 - \varepsilon))}} \\ &= \left(\frac{\sqrt{r(n_1 - r)} \|\tilde{S}\|_{2 \to 2}}{\sqrt{\delta_1}(\sqrt{r} - \sqrt{r_1} - \sqrt{\log(1/\delta_2)})} + \frac{\sqrt{r} \|S\|_{2 \to 2}}{\sqrt{\log(1/(1 - \varepsilon))}} + 1\right) \sigma_{r_1 + 1}(X_0) \\ &+ \frac{\sqrt{r(n_1 - r)} \|\tilde{Z}\|_{2 \to 2}}{\sqrt{\delta_1}(\sqrt{r} - \sqrt{r_1} - \sqrt{\log(1/\delta_2)})} + \frac{\sqrt{r} \|Z\|_{2 \to 2}}{\sqrt{\log(1/(1 - \varepsilon))}}. \end{split}$$

From concentration the of operator norm of  $\tilde{S}$  and S in Lemma 5, with probability  $1-2\delta_2$ , we have that

$$||S||_{2\to 2} \le \sqrt{r} + \sqrt{n_1} + \sqrt{\log(1/\delta_2)}, \quad ||\tilde{S}||_{2\to 2} \le \sqrt{r} + \sqrt{n_2} + \sqrt{\log(1/\delta_2)}.$$

We then obtain the desired bound.

Proof of Corollary 2. Consider the double sketch tensor approach described in (7):

$$\mathcal{Y} = \mathcal{S} * \mathcal{X}_0 + \mathcal{Z}, \ \ \tilde{\mathcal{Y}} = \tilde{\mathcal{S}} * \mathcal{X}_0^* + \tilde{\mathcal{Z}}$$

where  $S_1 = S$ ,  $\tilde{S}_1 = \tilde{S}$  and  $S_k = \tilde{S}_k = \mathbf{0}$  for all  $k \in \{2, ..., n_3\}$ . With this construction, after performing a mode-3 Fourier transformation (2) on the tensors, the measurements  $\hat{\mathcal{Y}}$  and  $\hat{\tilde{\mathcal{Y}}}$  can be decomposed into  $n_3$  low-rank matrix sketches:

$$\widehat{\mathcal{Y}}_{i} = \widehat{\mathcal{S}}_{i}\widehat{\mathcal{X}}_{0i} + \widehat{\mathcal{Z}}, \quad \widehat{\widetilde{\mathcal{Y}}}_{i} = \widehat{\widetilde{\mathcal{S}}}_{i} * \widehat{\mathcal{X}}_{0i}^{*} + \widehat{\widetilde{\mathcal{Z}}}_{i}, \quad i \in [n_{3}].$$

$$(16)$$

Notice that it follows from the definition of mode-3 Fourier transformation in (2),  $\widehat{\mathcal{S}}_1$  and  $\widehat{\mathcal{S}}_1$  are two complex Gaussian random matrices with independent entries by the unitary invariance of the complex Gaussian distribution. Thus, the results of Theorem 1 and Theorem 2 can be applied to produce recovery guarantees for the double sketch tensor approach. In particular, when  $\mathcal{Z} = \widetilde{\mathcal{Z}} = \mathbf{0}$ , by Theorem 1, each of the  $n_3$  transformed frontal slices  $\mathcal{X}_i$  can be recovered with probability 1 from the sketches given in (16).

For general noise, we start by noting that

$$\|\mathcal{X} - \mathcal{X}_0\|_F^2 = \sum_{k=1}^{n_3} \|\mathcal{X}_k - (\mathcal{X}_0)_k\|_F^2$$

$$\leq \sum_{k=1}^{n_3} 2\|\widehat{\mathcal{X}}_k - \overline{\widehat{\mathcal{X}}}_k\|_F^2 + 2\|\overline{\widehat{\mathcal{X}}}_k - (\widehat{\mathcal{X}}_0)_k\|_F^2,$$

where  $\widehat{\mathcal{X}}_k$ ,  $(\widehat{\mathcal{X}}_0)_k \in \mathbb{C}^{n_1 \times n_2}$  are  $k^{th}$  frontal slices of the the mode-3 FFT of  $\mathcal{X}$  and  $\widehat{\mathcal{X}}_0$ , and  $\overline{\widehat{\mathcal{X}}}_k$  is the recovered frontal slice in the noiseless setting. For the first term, we can use the same argument as in the proof of Theorem 2 and for the second term, we simply invoking Lemma 1. Thus, the approximation error is:

$$\begin{split} \|\mathcal{X} - \mathcal{X}_0\|_F^2 & \leq \sum_{k=1}^{n_3} 2\|\widehat{\mathcal{X}}_k - \overline{\widehat{\mathcal{X}}}_k\|_F^2 + 2\|\overline{\widehat{\mathcal{X}}}_k - (\widehat{\mathcal{X}}_0)_k\|_F^2 \\ & \leq \sum_{k=1}^{n_3} \frac{2r(n_1 - r)\|\widehat{\widehat{\mathcal{Z}}}_k\|_F^2}{\delta_1(\sqrt{r_1} - \sqrt{r} - \sqrt{\log(1/\delta_2)})^2} + \frac{2r\|\widehat{\mathcal{Z}}_k\|_F^2}{\log(1/(1 - \varepsilon))} \\ & \leq \frac{2r(n_1 - r)}{\delta_1(\sqrt{r_1} - \sqrt{r} - \sqrt{\log(1/\delta_2)})^2} \sum_{k=1}^{n_3} \|\widehat{\widehat{\mathcal{Z}}}_k\|_F^2 + \frac{2\sqrt{r}}{\log(1/(1 - \varepsilon))} \sum_{k=1}^{n_3} \|\widehat{\mathcal{Z}}_k\|_F^2 \\ & \leq \frac{2r(n_1 - r)}{\delta_1(\sqrt{r_1} - \sqrt{r} - \sqrt{\log(1/\delta_2)})^2} \|\widehat{\widehat{\mathcal{Z}}}\|_F^2 + \frac{2r}{\log(1/(1 - \varepsilon))} \|\widehat{\mathcal{Z}}\|_F^2 \\ & = \frac{2r(n_1 - r)\|\widehat{\mathcal{Z}}\|_F^2}{\delta_1(\sqrt{r_1} - \sqrt{r} - \sqrt{\log(1/\delta_2)})^2} + \frac{2r\|\mathcal{Z}\|_F^2}{\log(1/(1 - \varepsilon))}. \end{split}$$

## 4 Experiments

We complement our theoretical findings with numerical experiments examining the empirical behavior of the approximation error using the double sketch algorithm for recovering low-rank matrices from noise sketches.

10

In these experiments, we fix the dimension of the rank  $r_0$  matrix to be  $100 \times 100$ , initialized by multiplying two i.i.d. complex Gaussian matrices of size  $100 \times r_0$  and  $r_0 \times 100$ . Empirical approximation error represents the median error over 20 trials where the sketching matrices change with each trial. The entries of error matrices (or tensors) Z and  $\tilde{Z}$  (Z and  $\tilde{Z}$ ) are drawn i.i.d. from a standard Gaussian distribution and then normalized to achieve the desired norm. For these numerical experiments, all norms and errors are measured in the Frobenius norm.

Figure 1 demonstrates the performance of the double sketch algorithm for recovering a low-rank matrix when  $r_0 = 10$  and  $r \in \{r+1, 2r, n-1\}$  (left to right). For each tuple  $(r_0, r)$ , we plot the approximation error while varying the noise levels  $\epsilon_1 = ||Z||_F$  and  $\epsilon_2 = ||\tilde{Z}||_F$ . Going from left to right in Figure 1, we observe that the approximation error is robust with respect to  $\varepsilon_1$  when r is close to  $r_0$  and then transition to being robust with respect to  $\varepsilon_2$  when r approaches r. This is expected as the error bound represented in Theorem 2 depends on r. In particular, if we pick r = r, the error bound becomes independent of  $\varepsilon_2$ . Similarly, picking r close to  $r_0$ , the term involving of  $\varepsilon_2$  becomes the dominant term in the error bound.

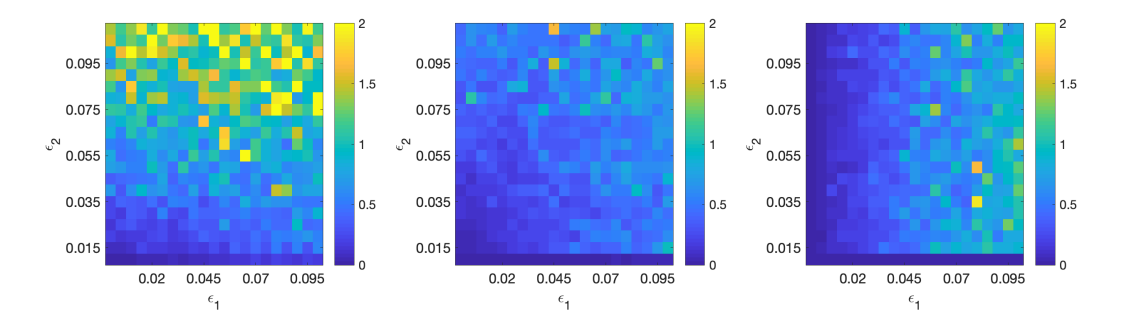


Figure 1: Numerical results demonstrating the empirical performance of the double sketching algorithm while varying  $||Z||_F = \varepsilon_1$  and  $||\tilde{Z}||_F = \varepsilon_2$  when n = 100, r = 10, and (left)  $r_1 = r + 1$  (center)  $r_1 = 2r$  (right)  $r_1 = n - 1$ .

In our next experiment, we consider the recovery of low-tubal-rank tensors. Figure 2 presents the empirical approximation errors obtained when using the double sketch algorithm 7 to recover low-tubal-rank tensors. To initialize the underlying low-rank tensor, we multiple two tensors of dimension  $n \times r \times n_3$  and  $r \times n \times n_3$ . Thus, the tubal rank of the tensor is r and  $\mathcal{X} \in \mathbb{R}^{n \times n \times n_3}$ . Similar to the experiment presented for the matrix case, the approximation error is the median error from 20 trails where new sketching matrices are drawn for each trial. We also vary both the choice of r and the size of the tensor  $n_3$ . In Figure 2, we can see that increasing  $n_3$  has no impact on the approximation error. Based on the upper bound shown in Corollary 2, this behavior is expected. We also obverse that as  $r_1$  approaches n, the double sketch method becomes more robust to the noise in  $\tilde{\mathcal{Z}}$ .

## 5 Conclusion

In this paper, we study the robust recovery of low-rank matrices and low-tubal-rank tensors from sketched matrices. Our main results show that, without making assumptions on the distribution of the noise Z and  $\tilde{Z}$ , one can reconstruct the low-rank matrix using the double sketch algorithm discussed in [24] with theoretical guarantees. This analysis is also applicable to low-tubal-rank tensor recovery. Numerical experiments support our theoretical results.

A possible extension is to analyze the truncated version of the noisy sketching algorithm in [24, 35] for low-rank approximation. It will also be interesting to see whether our analysis can be extended to the scenario when more structured sketching matrices such as subsampled randomized Hadamard transforms [5] are used. These more structured sketching matrices have the advantage of reducing the computational burden and the memory footprint compared to Gaussian sketching matrices. Note that while our deterministic formula

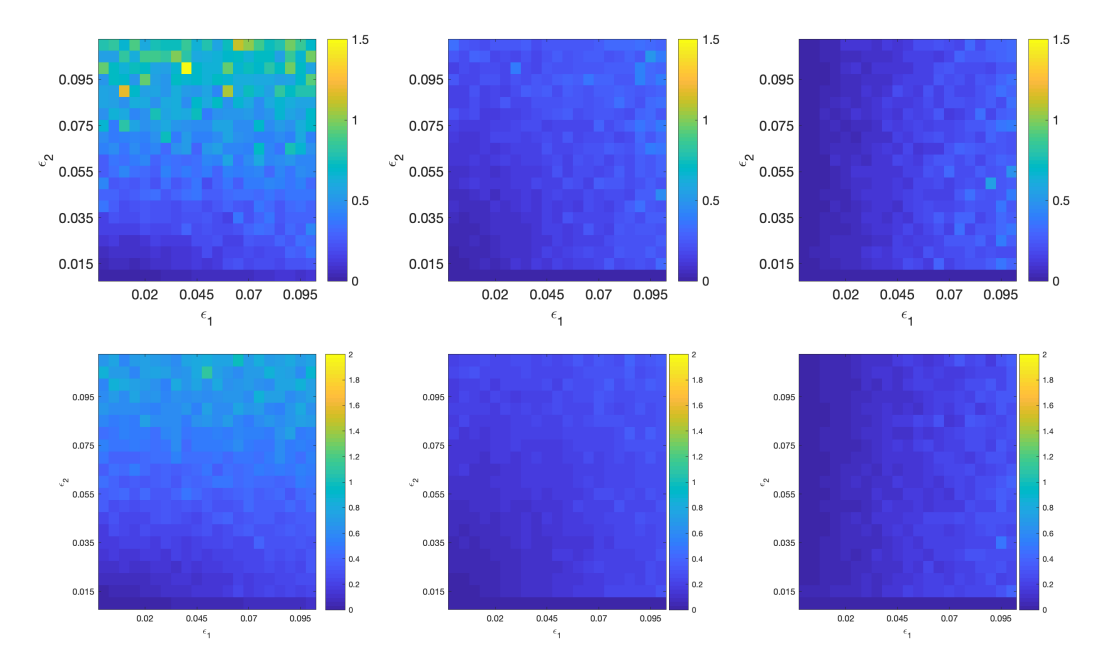


Figure 2: Numerical results demonstrating the empirical performance of the double sketching algorithm while varying  $\|\mathcal{Z}\|_F = \varepsilon_1$  and  $\|\tilde{\mathcal{Z}}\|_F = \varepsilon_2$  when n = 100, r = 10, (left column)  $r_1 = r + 1$  (center column)  $r_1 = 2r$  (right column)  $r_1 = n - 1$ . Each row presents the numerical results for different values of  $n_3$ : (first row)  $n_3 = 10$  and (second row)  $n_3 = 50$ .

for the difference between the output of the sketching algorithm and the ground truth matrix also holds in this setting, it is not known to us whether some of the involved concentration inequalities still hold in this scenario. We believe that this is an interesting avenue for future research.

## **Appendix**

**Lemma 2** (Properties of the pseudo-inverse, [14]). The following properties hold for pseudo-inverse.

- 1.  $(AB)^{\dagger} = B^{\dagger}A^{\dagger}$  if A has orthonormal columns or B has orthonormal rows.
- 2.  $(AB)^{\dagger} = B^{\dagger}A^{\dagger}$  if A has linearly independent columns  $(A^{\dagger}A = I)$  and B has linearly independent rows  $(BB^{\dagger} = I)$ .
- 3. If A has orthonormal columns or orthonormal rows, then  $A^{\dagger} = A^*$ .

**Lemma 3** (Oblique projection matrix, Theorem 2.1 in [15], see also Equation (7.10.40) in [21]). Let  $P \in \mathbb{C}^{n \times n}$  be a projection matrix, i.e.  $P^2 = P$ . We note that P is uniquely characterized by the subspaces  $V_1$  and  $V_2$  given by

$$V_1 := \operatorname{Im} P,$$

$$V_2 = \operatorname{Ker} P.$$

and dim  $V_1 + \text{dim } V_2 = n$ . By some abuse of notation, we denote by  $V_1$  a matrix with orthonormal columns, whose column span is equal to the subspace  $V_1$ . Analogously, we denote by  $V_2$  a matrix with orthonormal columns, whose column span is equal to the subspace  $V_2$ . It holds that

$$P = V_1(V_{2,\perp}^* V_1)^{-1} V_{2,\perp}^*.$$

**Lemma 4** (Smallest singular value of a truncated Haar unitary matrix, Proposition D.3 in [3]). Let A be the upper left  $(n-r) \times (n-r)$  corner of a Haar unitary matrix U. Then for any  $\delta > 0$ 

$$\mathbb{P}\left(\sigma_{\min}(A) \ge \frac{\sqrt{\delta}}{\sqrt{r(n-r)}}\right) \ge 1 - \delta.$$

**Lemma 5** (Extreme singular value of Gaussian random matrices, Corollary 5.35 in [31]). Let A be a random  $m \times n$  random matrix with independent standard complex Gaussian entries and m > n, then for any  $\delta > 0$ , with probability at least  $1 - \delta$ ,

$$\sigma_{\min}(A) \ge \sqrt{m} - \sqrt{n} - \sqrt{\log(1/\delta)}$$
.

Similarly, with probability at least  $1 - \delta$ ,

$$\sigma_{\max}(A) \le \sqrt{m} + \sqrt{n} + \sqrt{\log(1/\delta)}$$
.

*Proof.* This lemma was proved in [31] for real Gaussian matrices. We include a proof for complex Gaussian matrices for completeness. We have

$$\sigma_{\min}(A) = \min_{u \in S^{n-1}} \max_{v \in S^{m-1}} \langle Au, v \rangle,$$

where  $S^{n-1}$  is the unit sphere in  $\mathbb{C}^n$ . Let  $X_{u,v} = \langle Au, v \rangle$  and  $Y_{u,v} = \langle g, u \rangle + \langle h, v \rangle$ , where  $g \in \mathbb{C}^n$ ,  $h \in \mathbb{C}^m$  are independent standard complex Gaussian random vectors. We find for any  $x, w \in S^{n-1}$  and any  $y, z \in S^{m-1}$ ,

$$\mathbb{E}|X_{u,v} - X_{w,z}|^2 = \|uv^* - wz^*\|_F^2 \le \|u - w\|_2^2 + \|v - z\|_2^2 = \mathbb{E}|Y_{u,v} - Y_{w,z}|^2.$$

From Gordon's inequality ([32, Exercise 7.2.14]) and [32, Exercise 7.3.4],

$$\mathbb{E}\sigma_{\min}(A) \ge \mathbb{E}||h||_2 - \mathbb{E}||g||_2.$$

Since  $\mathbb{E}||g||_2 \le (\mathbb{E}||g||_2^2)^{1/2} = \sqrt{n}$ ,

$$\mathbb{E}\sigma_{\min}(A) \ge (\mathbb{E}||h||_2 - \sqrt{m}) + \sqrt{m} - \sqrt{n}.$$

We also have  $||h||_2^2 = \sum_{i=1}^m |h_i|^2 = \frac{1}{2}W$ , where  $W \sim \chi^2(2m)$ . So

$$\mathbb{E}||h||_2 - \sqrt{m} = \frac{1}{\sqrt{2}} \left( \mathbb{E}\sqrt{W} - \sqrt{2m} \right) \ge 0,$$

where the last inequality is due to the fact that  $f(n) = \mathbb{E}||g||_2 - \sqrt{n}$  is an increasing function in n, where  $g \sim N(0, I_n)$ , and  $||g||_2^2 \sim \chi^2(n)$ .

Since  $\sigma_{\min}(A)$  is a Lipschitz function of 2mn independent real Gaussian random variables with mean zero and variance 1/2, then the probability estimate follows from Gaussian concentration of Lipschitz functions (see [31, Proposition 5.34]). The largest singular value  $\sigma_{\max}(A)$  can be estimated in a similar way using the Sudakov-Fernique inequality [32, Theorem 7.2.11].

**Lemma 6** (Smallest eigenvalue of a square Gaussian random matrix, [10] and Theorem 1.1 in [28]). Let A be an  $n \times n$  complex standard Gaussian random matrix. Then

$$\mathbb{P}\left(\sigma_{\min}(A) \ge \varepsilon n^{-1/2}\right) = e^{-\varepsilon^2}.$$

## References

- [1] Martin Azizyan, Akshay Krishnamurthy, and Aarti Singh. Extreme compressive sampling for covariance estimation. IEEE Trans. Inf. Theory, 64(12):7613–7635, 2018.
- [2] Grey Ballard, James Demmel, Ioana Dumitriu, and Alexander Rusciano. A generalized randomized rank-revealing factorization. arXiv preprint arXiv:1909.06524, 2019.
- [3] Jess Banks, Jorge Garza-Vargas, Archit Kulkarni, and Nikhil Srivastava. Pseudospectral shattering, the sign function, and diagonalization in nearly matrix multiplication time. In <u>2020 IEEE 61st Annual Symposium</u> on Foundations of Computer Science (FOCS), pages 529–540. IEEE, 2020.
- [4] Ayan Kumar Bhunia, Subhadeep Koley, Abdullah Faiz Ur Rahman Khilji, Aneeshan Sain, Pinaki Nath Chowdhury, Tao Xiang, and Yi-Zhe Song. Sketching without worrying: Noise-tolerant sketch-based image retrieval. arXiv preprint arXiv:2203.14817, 2022.
- [5] Christos Boutsidis and Alex Gittens. Improved matrix algorithms via the subsampled randomized Hadamard transform. SIAM J. Matrix Anal. Appl., 34(3):1301–1340, 2013.
- [6] Venkat Chandrasekaran, Benjamin Recht, Pablo A Parrilo, and Alan S Willsky. The convex geometry of linear inverse problems. Found. Comput. Math., 12(6):805–849, 2012.
- [7] Yuxin Chen, Yuejie Chi, Jianqing Fan, and Cong Ma. Spectral methods for data science: A statistical perspective. Foundations and Trends® in Machine Learning, 14(5):566–806, 2021.
- [8] Chandler Davis and William Morton Kahan. The rotation of eigenvectors by a perturbation. iii. <u>SIAM</u> J. Numer. Anal., 7(1):1–46, 1970.
- [9] Ioana Dumitriu. Smallest eigenvalue distributions for two classes of  $\beta$ -jacobi ensembles. <u>J. Math. Phys.</u>, 53(10):103301, 2012.
- [10] Alan Edelman. Eigenvalues and condition numbers of random matrices. SIAM J. Matrix Anal. Appl., 9(4):543–560, 1988.
- [11] Alan Edelman and Brian D Sutton. The beta-Jacobi matrix model, the CS decomposition, and generalized singular value problems. Found. Comput. Math., 8(2):259–285, 2008.
- [12] Jon Elerath. Hard-disk drives: The good, the bad, and the ugly. <u>Communications of the ACM</u>, 52(6):38–45, 2009.
- [13] Maryam Fazel, E Candes, Benjamin Recht, and P Parrilo. Compressed sensing and robust recovery of low rank matrices. In 2008 42nd Asilomar Conference on Signals, Systems and Computers, pages 1043–1047. IEEE, 2008.
- [14] G.H. Golub and C.F. Van Loan. <u>Matrix Computations</u>. Johns Hopkins Studies in the Mathematical Sciences. Johns Hopkins University Press, 2013.
- [15] Per Christian Hansen. Oblique projections, pseudoinverses, and standard-form transformations. Technical University of Denmark, Tech. Rep., 2004.
- [16] Botao Hao, Anru R Zhang, and Guang Cheng. Sparse and low-rank tensor estimation via cubic sketchings. In <u>International Conference on Artificial Intelligence and Statistics</u>, pages 1319–1330. PMLR, 2020.
- [17] Eric Kernfeld, Misha Kilmer, and Shuchin Aeron. Tensor-tensor products with invertible linear transforms. Linear Algebra Appl., 485:545–570, 2015.

- [18] Misha E Kilmer, Karen Braman, Ning Hao, and Randy C Hoover. Third-order tensors as operators on matrices: A theoretical and computational framework with applications in imaging. SIAM J. Matrix Anal. Appl., 34(1):148–172, 2013.
- [19] Canyi Lu, Jiashi Feng, Yudong Chen, Wei Liu, Zhouchen Lin, and Shuicheng Yan. Tensor robust principal component analysis with a new tensor nuclear norm. <u>IEEE transactions on pattern analysis</u> and machine intelligence, 42(4):925–938, 2019.
- [20] Canyi Lu, Jiashi Feng, Zhouchen Lin, and Shuicheng Yan. Exact low tubal rank tensor recovery from gaussian measurements. In <u>Proceedings of the 27th International Joint Conference on Artificial Intelligence</u>, pages 2504–2510, 2018.
- [21] Carl D. Meyer. Matrix analysis and applied linear algebra. Philadelphia, PA: Society for Industrial and Applied Mathematics (SIAM), 2000.
- [22] Sean O'Rourke, Van Vu, and Ke Wang. Random perturbation of low rank matrices: Improving classical bounds. Linear Algebra Appl., 540:26–59, 2018.
- [23] Liqun Qi and Gaohang Yu. T-singular values and t-sketching for third order tensors. arXiv preprint arXiv:2103.00976, 2021.
- [24] Benjamin Recht, Maryam Fazel, and Pablo A. Parrilo. Guaranteed minimum-rank solutions of linear matrix equations via nuclear norm minimization. SIAM Rev., 52(3):471–501, 2010.
- [25] Mark Rudelson and Roman Vershynin. Non-asymptotic theory of random matrices: extreme singular values. In <u>Proceedings of the International Congress of Mathematicians 2010 (ICM 2010) (In 4 Volumes)</u> <u>Vol. I: Plenary Lectures and Ceremonies Vols. II–IV: Invited Lectures, pages 1576–1602. World Scientific, 2010.</u>
- [26] Rakshith Sharma Srinivasa, Kiryung Lee, Marius Junge, and Justin Romberg. Decentralized sketching of low rank matrices. In H. Wallach, H. Larochelle, A. Beygelzimer, F. d'Alché-Buc, E. Fox, and R. Garnett, editors, Advances in Neural Information Processing Systems, volume 32. Curran Associates, Inc., 2019.
- [27] Yiming Sun, Yang Guo, Charlene Luo, Joel Tropp, and Madeleine Udell. Low-rank tucker approximation of a tensor from streaming data. SIAM Journal on Mathematics of Data Science, 2(4):1123–1150, 2020.
- [28] Terence Tao and Van Vu. Random matrices: The distribution of the smallest singular values. <u>Geom. Funct. Anal.</u>, 20(1):260–297, 2010.
- [29] Joel A. Tropp, Alp Yurtsever, Madeleine Udell, and Volkan Cevher. Practical sketching algorithms for low-rank matrix approximation. SIAM J. Matrix Anal. Appl., 38(4):1454–1485, 2017.
- [30] Joel A. Tropp, Alp Yurtsever, Madeleine Udell, and Volkan Cevher. Streaming low-rank matrix approximation with an application to scientific simulation. <u>SIAM J. Sci. Comput.</u>, 41(4):a2430–a2463, 2019.
- [31] Roman Vershynin. <u>Introduction to the non-asymptotic analysis of random matrices</u>, page 210–268. Cambridge University Press, 2012.
- [32] Roman Vershynin. High-dimensional probability: An introduction with applications in data science, volume 47. Cambridge university press, 2018.
- [33] Hailin Wang, Feng Zhang, Jianjun Wang, Tingwen Huang, Jianwen Huang, and Xinling Liu. Generalized nonconvex approach for low-tubal-rank tensor recovery. IEEE Trans. Neural Netw. Learn. Syst., 2021.
- [34] Per-Åke Wedin. Perturbation bounds in connection with singular value decomposition. <u>BIT</u>, 12(1):99–111, 1972.

- [35] Franco Woolfe, Edo Liberty, Vladimir Rokhlin, and Mark Tygert. A fast randomized algorithm for the approximation of matrices. Appl. Comput. Harmon. Anal., 25(3):335–366, 2008.
- [36] Qianxin Yi, Chenhao Wang, Kaidong Wang, and Yao Wang. Effective streaming low-tubal-rank tensor approximation via frequent directions. arXiv preprint arXiv:2108.10129, 2021.
- [37] Feng Zhang, Wendong Wang, Jingyao Hou, Jianjun Wang, and Jianwen Huang. Tensor restricted isometry property analysis for a large class of random measurement ensembles. <u>Science China Information</u> Sciences, 64(1):1–3, 2021.
- [38] Feng Zhang, Wendong Wang, Jianwen Huang, Jianjun Wang, and Yao Wang. Rip-based performance guarantee for low-tubal-rank tensor recovery. <u>Journal of Computational and Applied Mathematics</u>, 374:112767, 2020.
- [39] Zemin Zhang and Shuchin Aeron. Exact tensor completion using t-SVD. <u>IEEE Trans. Signal Process.</u>, 65(6):1511–1526, 2016.
- [40] Tianyi Zhou and Dacheng Tao. Bilateral random projections. In <u>2012 IEEE International Symposium</u> on Information Theory Proceedings, pages 1286–1290. IEEE, 2012.